Published in final edited form as:
J Am Soc Echocardiogr. 2013 August ; 26(8): 910–918. doi:10.1016/j.echo.2013.04.016.

Comparison of echocardiographic measurements of left ventricular volumes to full volume magnetic resonance imaging in normal and diseased rats

Teresa Arias, PhD[1,2], **Jiqiu Chen, MD**[1], **Zahi A. Fayad, PhD**[1], **Valentin Fuster, MD, PhD**[1,2], **Roger J. Hajjar, MD**[1], and **Elie R. Chemaly, MD, PhD**[1,*]

[1]Zena and Michael A. Wiener Cardiovascular Institute, Icahn School of Medicine at Mount Sinai, One Gustave L. Levy Place, Box 1030, New York, NY, 10029, USA

[2]Centro Nacional de Investigaciones Cardiovasculares (CNIC), Melchor Fernández Almagro, 3, Madrid, 28029, Spain

Abstract

Background—Clinical two-dimensional (2D) and clinical three-dimensional (3D) echocardiography are validated against Cardiac Magnetic Resonance imaging (CMR), the gold standard for left ventricle (LV) volumes. In rodents, there is no widely accepted echocardiographic measure of whole LV volumes, and CMR measurements vary between studies. We compared LV volumes by 2D-echocardiography (hemisphere-cylinder (HC) model) to HC and full-volume (FV) CMR in normal and diseased rats to measure the impact of geometric models and imaging modalities.

Methods—Rats (n=27) underwent ascending aortic banding, myocardial infarction induction by either permanent left anterior descending artery (LAD) ligation or ischemia-reperfusion, and sham thoracotomy. Subsequently, we measured end-diastolic volume (EDV), end-systolic volume (ESV) and ejection fraction (EF) using a HC-2D-echocardiography model combining parasternal short-axis and long-axis measurements and compared these to HC and FV-CMR.

Results—Diseased groups showed LV dilatation and dysfunction. HC-echocardiography and FV-CMR measures of EDV, ESV and EF were correlated. On Bland-Altman plots, EDV were concordant between both methods while HC-echocardiography underestimated ESV, resulting in a modest overestimation of EF versus FV-CMR. Other 2D-echocardiographic geometric models offered less concordance with FV-CMR than HC. HC-CMR overestimates LV volumes versus FV-CMR, while HC-echocardiography underestimates HC-CMR volumes. Echocardiography underestimates corresponding LV dimensions by CMR, particularly short-axis.

Conclusions—Concordant measures of LV volume and function were obtained using: (1) a relatively simple HC model of the LV inclusive of two orthogonal 2D-echocardiographic planes,

*Corresponding author: Elie R. Chemaly MD, PhD, Zena and Michael A. Wiener Cardiovascular Institute, Icahn School of Medicine at Mount Sinai, One Gustave L. Levy Place, Box 1030, New York, NY, 10029, USA, Work phone: 1-212-824-8908, Fax: 1-212-241-4080, elie.chemaly@mssm.edu.

Disclosures:
The authors do not have any conflict of interest pertinent to this manuscript.

and (2) FV-CMR in normal and diseased rats. The HC model appears to compensate the underestimation of LV dimensions by echocardiography.

Keywords

Echocardiography; magnetic resonance imaging; rat; animal ultrasound; animal models of disease

Introduction

Echocardiography and Cardiac Magnetic Resonance Imaging (CMR) measure left ventricle (LV) volumes and function. In humans, full-volume (FV) CMR is the gold standard for LV size and function due to its ability to obtain three-dimensional (3D) images of the LV and thus measure LV volumes without geometric assumptions [1]. In small animals, FV-CMR is gaining momentum for similar reasons[2].

Both echocardiography and CMR are complementary techniques with advantages and disadvantages[2, 3], but little is known about the comparability of their volume measurements in rodents, and their comparative ability to detect small and large variations in LV size and function.

On the other hand, several published echocardiographic indicators of LV dimension used in rodents rely exclusively on a single parasternal short-axis or long-axis view, with or without M-mode imaging[4-7], and often derive LV volumes from monodimensional measures[7, 8].

The need for 3D measurements of LV size and function using rodent echocardiography has been understood for a long time[4], but no approach is recognized as standard and optimal in that regard. Real-time 3D echocardiography is now widely used in humans [1, 9]; 3D echocardiography has been successfully performed in rodents[10-12] but remains of limited availability and applicability, with some technical challenges such as the need for gated imaging[11, 12]. Besides, real-time 3D echocardiography requires matrix array transducers[13] which, to our knowledge, are not developed for small animal use. Real-time 3D echocardiography is still constrained by lower spatial resolution and frame rate compared to 2D echocardiography, which further limits its application to small animals[9]. Thus, for small animal imaging, it remains useful to determine the most suitable 2D echocardiography-based geometric model to determine LV volumes.

Picard MH et al. have reviewed and discussed the importance of 3D echocardiography and the limitations of geometric models of LV volumes from 2D echocardiographic views[13]. One such measure of LV volumes uses the “bullet formula”, or hemisphere-cylinder (HC) model, as reported in rat studies using echocardiography [14, 15] and CMR[16]. This geometric model has the theoretical advantage of including 3 dimensions of the LV by combining cross-sectional area of the parasternal short-axis view (2 dimensions) with cavity length from the parasternal long-axis view (a third perpendicular dimension); it was validated in dogs[17] and recommended for echocardiographic LV volume and LV mass calculation in humans[18]. Another advantage of the HC model is its entire reliance on parasternal views, which are easier to obtain with the high-resolution linear-array probes commonly used in rodents, and less subject to foreshortening than apical views in rodents.

We compared LV volumes by 2D-echocardiography in rats using a HC model to HC and FV-CMR in two disease models of rat LV dysfunction and dilatation of graded severity.

Methods

Animal use and care

Animals were obtained and handled as approved by the Institutional Animal Care and Use Committee of the Icahn School of Medicine at Mount Sinai in accordance with the "Principles of Laboratory Animal Care by the National Society for Medical Research and the Guide for the Care and Use of Laboratory Animals" (National Institutes of Health Publication No. 86-23, revised 1996).

Surgical animal disease models

We studied 27 rats. Male Sprague-Dawley rats (200-250 grams) underwent surgery as previously described[19]. Pressure-overload LV hypertrophy (POH) and failure was induced by ascending-aortic banding (n=4), and myocardial infarction (MI) was created by permanent left anterior descending artery (LAD) ligation (n=9), or LAD ligation for 30 minutes followed by reperfusion (n=5) [19]. Sham animals underwent a thoracotomy without MI or aortic constriction (n=4), and normal animals (n=5) of similar age and weight at the time of imaging were used.

One to two months after surgery, animals underwent consecutive echocardiography and CMR by double-blinded operators and in random order. The time interval between CMR and echocardiography on the same animal was 0±5 days.

Echocardiography

Echocardiography was performed under sedation by intraperitoneal ketamine up to 80mg/kg, with starting doses as low as 10mg given to diseased rats and supplemented by additional injections until optimal sedation was obtained. Sedation was optimized by giving the lowest dose of ketamine needed to (1) restrain the animal and prevent motion artifact (2) maintain the heart rate in the range of 350-450 beats/minute. Ketamine was chosen based on our previous experience and considering that alternative agents had either a long duration of action (pentobarbital), potentially unsafe for heart failure animals, or a bradycardic effect (isoflurane, ketamine/xylazine) as demonstrated elsewhere[20]. The chest was shaved.

Short-axis parasternal views of the LV at the mid-papillary level and long-axis parasternal views of the LV were obtained using a Vivid i echocardiography apparatus with a 13MHz linear array probe (General Electric, New York, NY) at a frame rate ranging from 25 to 28 frames/second for 2D echocardiography. Volumes of the LV cavity at end-diastole and end-systole were calculated using an area-length hemisphere-cylinder (HC) formula that assumes a bullet-shaped LV as previously recommended and described[15]. LV end-diastolic and end-systolic volumes (respectively EDV and ESV) were thus calculated as follows: $V=5/6\times A\times L$ where V is the volume of the LV cavity in ml, A is the cross-sectional area of the LV cavity in cm^2 obtained from a parasternal short-axis image at the mid-papillary level, and L is the length of the LV cavity in cm measured as the distance from the endocardial LV apex to the mitral-aortic junction on the parasternal long-axis image as previously described[15, 17, 18]. Additional planimetry was performed on the parasternal long-axis view to obtain LV volumes (1) by application of a modified Simpson's rule (programmed in the software package of the ultrasound device) (2) by measurement of the area A and length L of the echocardiographic long-axis modeled as a single plane ellipsoid in which LV volume = $(8A^2)/(3\pi L)$ as previously published[7, 16].

M-mode echocardiography was performed on short-axis parasternal views as previously recommended to obtain LV end-diastolic and end-systolic diameters[18]. The frame rate for M-mode echocardiography was 48 frames/second.

In 2D and M-mode LV cavity measurements, care was taken to exclude papillary muscles from the LV wall.

Magnetic resonance (MR) imaging

Rats were sedated with 1.5-2% of isoflurane in oxygen (0.6 liter/min), consistent with previous reports[8]. The respiratory rate was monitored using an MR-compatible monitoring system (SA Instruments, New York, NY) and maintained in the range of 55-70 breaths/min.

A 7 T horizontal bore animal MR scanner (Bruker BioSpin GmbH, Ettlingen, Germany) with 86mm RF volume coil (Bruker BioSpin) and Paravision 5.1 software was used. Following axial, sagittal and coronal localizer sequences the coil was tuned and matched. Then, bright blood cine images of 2, 3, and 4 chamber views of the LV were obtained using a retrospectively self-gated protocol (IntraGate, Bruker BioSpin). Acquisition parameters were as follow: echo time (TE): 2.96 ms, repetition time (TR): 9.8 ms; flip angle: 15°; field of view (FOV): 50 × 50 mm^2; matrix-size: 256 × 256; number of repetitions (NR): 200; cardiac frames reconstructed: 20; slice thickness: 1mm and scan time ~ 3min.

Full-volume (FV) imaging was also acquired using a retrospectively self-gated protocol with a 3D imaging volume (3D IntraGate, Bruker BioSpin) and the additional acquisition of navigator echoes[21]. Short-axis orientation was defined using the 3 chamber and the 4 chamber views as shown in Figure 1. The navigator slice was placed above the 3D imaging package that covered the LV cavity from base to apex. Sequence parameters were as follows: radiofrequency pulse (RF): 1 ms sinc pulse (10 lobes, bandwidth: 20 kHz); slab thickness: 10 mm, 10 mm; FOV: 50 × 50 × (18-14) mm^3; Nx × Ny × Nz: 128 × 128 × (12-9); spatial resolution: 0.312 × 0.312 × 1.5 mm/pixel; TE: 2 ms; TR: 8 ms; number of repetitions (NR): 50 and flip angle α: 14°; On navigator slice: RF pulse: 1 ms Gauss pulse (bandwidth: 2.740 kHz); slice thickness: 3.9 mm and flip angle α^{nav}: 8°. No more than 70% of all k-lines were used for the reconstruction of 16 cardiac time frames to avoid artifacts from respiratory movement. Total scan time was ~ 8-10 min (Ny × Nz × TR/NR). The effective number of averages was approximately 2.5 (70% × NR/6).

Analysis of global LV function was calculated using Segment software (Segment 1.9, Medviso, Sweden). Myocardium segmentation was performed among at least 7 LV short-axis slices outlining both, endocardial and epicardial borders in all the cardiac frames (Figure 1). EDV and ESV were calculated from the largest and smallest areas, respectively, of the LV cavity in each slice. Apical and basal slices without semicircular muscular ring at either end-systole or end-diastole were disregarded. Papillary muscles were not included in the LV wall, and the LV outflow tract was not included in the LV cavity in FV measurements.

Additional analysis of the CMR images included measurements similar to the ones performed by echocardiography on the long-axis and mid-papillary short-axis views, obtained using the CMR localizer sequences, and used to derive CMR volumes by the HC formula, as well as LV diameters from the short axis mid-papillary view (see above methods section on echocardiography for details).

Animal group assignment

Animals were divided into 5 groups: normal rats, sham-operated rats (thoracotomy, no MI and no POH), POH rats, rats with apical MI visible on all echocardiographic and CMR views, rats with small apical MI (visible on some but not all echocardiographic and/or CMR views).

Statistical analysis

Comparison of continuous variables between animal groups used the analysis of variance (ANOVA) followed by post-hoc pairwise comparisons using Student's t-test with Bonferroni correction for multiple testing. Concordance between LV volumes and EF by echo vs. CMR was measured using paired t-tests, Pearson's correlation on scatter-plots and Bland-Altman plots[22]. Linear regression of between-methods difference vs. among-methods average was performed on the Bland-Altman plot to test the hypothesis that the difference between the two methods did not vary across the range of measured values. Concordance between methods was quantified separately in diseased (n=18) and non-diseased (normal and sham, n=9) animals. A repeated-measurements ANOVA was used to compare sequential echocardiography and CMR-derived parameters across groups, for the purpose of testing a method-group interaction. This interaction tests the differential ability of the 2 methods to distinguish groups. Results are expressed as mean±standard deviation (SD). A p value of <0.05 was considered statistically significant. Stata 10.1 (Stata Corp, College Station, TX) was used for statistical analyses.

Results

Heart rate during imaging

Heart rate per animal group is shown in Table 1. It was significantly higher in echocardiography compared to CMR (394±53 beats/minutes vs. 294±54 beats/minutes; $p<0.0001$ for paired t-test).

Concordance and correlation of LV volumes and EF by HC-echocardiography and CMR (HC-CMR and FV-CMR)

Representative images of long-axis and short-axis views of the LV by echocardiography and CMR are shown in Figure 2, from the same sham and post-MI animals respectively. LV volumes (EDV and ESV) and EF measured by HC-echocardiography, HC-CMR and FV-CMR are shown in Table 1. Diseased groups demonstrated variable LV dilatation and dysfunction, most significant in the apical MI group (Table 1).

The agreement between HC-echocardiography and FV-CMR for the measurement of EDV, ESV and EF was assessed by paired t-tests (Table 2), Bland-Altman plots (Figure 3), and linear regression (scatter-plots shown in Figure 4).

Overall, HC-echocardiography and FV-CMR gave concordant measures of EDV (Table 2, Figure 3). The average difference in EDV between HC-echocardiography and FV-CMR was −8±123μl.

Compared to FV-CMR, HC-echocardiography underestimated ESV across its entire range, with an average HC-echocardiography-FV-CMR difference of −55±88μl (Table 2, Figure 3). This resulted in echocardiography overestimating EF by 10±12% (Table 2, Figure 3).

Agreement between volume measurement: differential impact of imaging modalities and geometric models

Compared to FV-CMR, HC-CMR overestimated EDV and ESV (Table 2). Moreover, HC-echocardiography underestimated volumes when compared to HC-CMR, indicating that the HC model per se overestimates LV volumes compared to the FV used as a reference, while echocardiography per se may underestimate LV volumes compared to CMR. EF was significantly different between the 3 methods (Table 2, Figure 3).

LV dimensions by echocardiography underestimate corresponding CMR dimensions

This underestimation is major for the short-axis area (Table 3), and for LV diameters of the mid-papillary short-axis view (data not shown). Short-axis diameters are consistently and severely underestimated by M-mode echocardiography compared to CMR short-axis diameters as well (data not shown).

In contrast, long-axis length was mildly underestimated by echocardiography at end-diastole and concordant at end-systole compared to CMR (Table 3). This better concordance in long-axis length suggested that LV volume geometric models relying solely on the long-axis view might generate values for LV volumes closer to FV-CMR. Nevertheless, when a modified single-plane Simpson was applied to the long-axis echocardiographic view alone, agreement for ESV with FV-CMR was not improved with regard to the underestimation by HC-echocardiography, and EDV was significantly underestimated compared to FV-CMR (in sharp contrast with the agreement offered by HC-echocardiography); the same observation was made using a the area A and length L of the echocardiographic long-axis to obtain LV volumes using a single plane ellipsoid model in which LV volume = $(8A^2)/(3\pi L)$ as previously published[7, 16] (Table 4).

Thus, when both EDV and ESV are taken into account in control and diseased animals, HC delivered values of LV volumes closest to FV-CMR among usual 2D-based echocardiographic models of LV volumes in rats.

Correlation and linear regression

EDV, ESV and EF showed significant correlation between the 2 modalities (HC-echocardiography and FV-CMR) in the overall sample (Figure 4). EDV and ESV were also significantly correlated in the subgroup of diseased animals, and ESV displayed significant correlation between both modalities in the subgroup of non-diseased animals. Correlations for EDV, ESV and EF in diseased and control subgroups as well as the overall sample were tested between the corresponding parameters and within the subgroups shown in Table 2 (data not shown). When the correlations shown in Figure 4 were taken as a reference, these tests revealed that intra-parameter correlation consistently improved when the same imaging modality was used (i.e. CMR with HC model correlated to FV-CMR) but did not consistently improve when the same geometric model was used with two imaging modalities (i.e. HC model by echocardiography versus HC model by CMR) (data not shown).

Thus, the disagreement between measurements as assessed by correlation appears to be mostly due to the disagreement between imaging modalities.

Comparative ability of HC-echocardiography and FV-CMR to discriminate between diseased and non-diseased animal groups

A repeated measurement ANOVA was performed with each one of the 3 parameters of interest (EDV, ESV, EF) as the dependent variable, with the animal group (Table 1) and the imaging modality (HC-echocardiography vs. FV-CMR) as the independent variables, in addition to a group-method interaction term. This test did not show a significant method-group interaction, indicating no significant difference between HC-echocardiography and FV-CMR in their ability to discriminate between animal disease models. A second analysis was performed in which a reference value for EDV, ESV and EF was taken as the average of the control group (Table 2). Changes from this reference value as detected by HC-echocardiography was compared to the change detected by FV-CMR within the specific diseased groups presented in Table 1. As shown in Table 5, only the reduction in EF in the small apical MI group was significantly larger when measured by HC-echocardiography,

while the two imaging approaches did not differ significantly in their performance otherwise.

Discussion

We demonstrate that an easy to use hemisphere-cylinder (HC) 2D-echocardiographic model of whole LV volume in rats provides measurements of LV size and function which (1) are well-correlated to full-volume (FV) CMR in both normal and diseased animals (2) fall in the same range as FV-CMR absolute measurements, particularly for EDV and (3) compare favorably to FV-CMR in their ability to discriminate between disease models of variable severity. We also show that echocardiography per se underestimates corresponding CMR measurements, in agreement with the recent human study by Greupner et al.[1]. In our study, this was mainly due to an underestimation of short-axis dimensions (Table 3). Interestingly, the geometric HC model per se, when applied on CMR images, leads to a major overestimation of LV volumes with an overall preserved agreement for EF (Tables 1 and 2). Conversely, since echocardiography per se appeared to underestimate corresponding LV dimensions and volumes compared to CMR, the agreement between HC-echocardiography and FV-CMR is a likely algebraic sum of these two opposing effects.

One theoretical strength of the HC volumetric model of LV echocardiography is to combine two orthogonal 2D planes, thus including 3 geometric dimensions in the volume measurements. Besides, it is now recognized that LV contraction and relaxation result in twisting and untwisting of the LV around its longitudinal axis[23]; thus, a 2D model of LV ejection like the HC that accounts for longitudinal shortening and short-axis area contraction is likely to provide more accurate measurements than most alternative 2D models routinely used in rodents which rely on single-plane or single-dimension measurements.

To our knowledge, this is the first study to compare the HC model of the LV obtained by echocardiography to FV-CMR, in normal and diseased rats. Previously, a measurement of LV cross-sectional area and derived ejection fraction (EF) in normal and infarcted rat hearts was compared to CMR-measured area and to CMR-derived full-volume EF[24]. The problem of echocardiographic LV volume measurement in rodents is ideally solved by real time 3D echocardiography, now in clinical use[1, 9]; however, and to our knowledge, currently available rodent 3D echocardiography does not involve real time imaging systems[12]. Indeed, few studies have evaluated 3D echocardiography in rodents. 3D reconstructions of mouse LV from multiple stacked short-axis images taken serially were obtained in normal and infarcted mice[10], and one study showed excellent agreement between murine 3D echocardiography and CMR[11]. Nevertheless, the difficulty of obtaining serial parallel short-axis views on rodents, and the need for gated ultrasound images[11, 12], have probably limited the use of rodent 3D echocardiography. Therefore, the determination of LV volumes from 2D images remains a widely used approach in rodent echocardiography, and even a proposed methodological “shortcut” in rodent CMR[16].

A recent study has shown variable agreement between various geometric models applied on CMR images from mouse and rat LV and FV-CMR measurements[16]; in that study, Simpson’s rule appeared to be superior to other 2D-based models. Simpson’s formula was applied on apical echocardiographic views in rodents[25], however, in our experience, apical views in rodents are foreshortened. Besides, whole LV volume measurements in three dimensions using Simpson’s rule requires 2 orthogonal and longitudinal planes of the LV, an approach of limited feasibility in rodent echocardiography. In the present study, a modified Simpson’s rule applied on the echocardiographic long-axis view of the LV underestimated EDV compared to FV-CMR, while HC-echocardiography provided

concordant EDV values, and ESV underestimation seen with HC-echocardiography persisted overall when the modified Simpson's rule was used (Table 4).

The amount of LV dilatation and dysfunction was modest in our study when compared to other works involving rats with MI[2]. However, our ability to show a significant correlation between the two methods in parameters that were varied over a relatively narrow range strengthens our results and shows both imaging methods to be similarly sensitive in our hands.

When LV dilatation and dysfunction were measured by both methods as the difference between the measurements in diseased animal and control values, overall testing, notably by repeated measurements ANOVA, showed a similar discriminatory ability for both methods, except in the group of animals with a small apical MI where HC-echocardiography detected a larger reduction of EF than FV-CMR (Table 5). All the differentiating factors between the techniques we discussed above and below can be invoqued to explain this particular result. This finding is consistent with the study by Xu et al.[26] showing that measuring LV function under more profound sedation can blur the detection of LV dysfunction. Interestingly, in our study, echocardiography with HC model appeared to be more sensitive than CMR-FV only when subtle LV dysfunction was considered (Table 5).

Limitations

One limitation of our study is the choice of anesthesia. We used ketamine for echocardiography and isoflurane for CMR, so that each imaging modality was performed under optimized and standard conditions. The use of different anesthetics is reflected in the differences in heart rates seen between the two imaging modalities; this may contribute at least in part to the differences in LV ejection fraction and dimension.

In rat echocardiography, our results in terms of LV function on ketamine[15, 27] were higher than previous reports using ketamine and xylazine[25]. It has been shown that either a combination of ketamine/xylazine or isoflurane caused a relatively significant bradycardia and reduced function in rats compared to low dose pentobarbital[20]; our echocardiographic data using ketamine are close to the published results in rats on low-dose pentobarbital and in conscious rats[20]. Ketamine is less costly than pentobarbital, and ketamine's shorter duration of action makes it safer for diseased rats than pentobarbital[20]. Besides, in mouse echocardiography, ketamine alone was shown to be a better agent than combined ketamine/xylazine[26].

Other studies have compared echocardiography and CMR using a different anesthesia regimen for each of the two modalities in rodents. Bunck et al. used a clinical 3T CMR scanner on normal mice and compared full volume LV size to echocardiographic volumes calculated using the Teichholz formula on M-mode measurements[8]. In that setting, they obtained comparable results from the two modalities using 0.3-0.8% isoflurane for echocardiography and 1-2% for CMR[8]. Comparability between the two imaging modalities used in our study would have been enhanced by performing both imaging studies with the same anesthesia. However, the short duration of action of ketamine, along with its superficial sedation, would have made it unpractical for the prolonged CMR. On the other hand, for full comparability to be achieved, echocardiography needed to be performed after prolonged sedation with isoflurane, thus administering isoflurane for durations that match what has been used in the CMR. Although rodent echocardiography is often performed under isoflurane sedation, it is seldom performed after prolonged administration of isoflurane. Therefore, while sacrificing some of the scientific comparability between methods, our protocol assures that both imaging modalities are used and compared in the conditions in which most investigators would use them. We believe this latter feature of our

study enhances the practical usefulness of our results. The relevance of further studies is certain in terms of refining the comparisons we performed; they need to be designed to specifically subtract or eliminate the impact of the anesthesia regimen ion the discrepancy between techniques.

A second limitation of our study is the practical difference in the measurement of the size (area and diameter) of the LV cavity by echocardiography and CMR. Papillary muscles were excluded from the LV wall in CMR and care was taken to exclude papillary muscles from the LV wall in echocardiography. However, due to the limited tissue definition of echocardiography and the small cavity size at end-systole in healthy control rats, it is not possible to assure the exclusion of papillary muscles in end-systolic measurements. This may contribute to the underestimation of ESV by echocardiography compared to CMR. The difficulty in excluding papillary muscles from the LV wall in small animal echocardiography, and particularly in end-systolic measurements, was also noted by the authors of a recent study on mice[7]. In addition, the variable inclusion of LV trabeculæ in the cavity is another known explanation for the differences between echocardiography and CMR measurements[13], however, we are unable to quantify precisely the role of this factor in our study. Time resolution was different between echocardiography and CMR, as reflected in the lower frame rate of echocardiography. Different frame rates affect the capture of the maximal (EDV) and minimal (ESV) ventricular volumes. Other sources of disagreement include the comparison of a real-time imaging technique (echocardiography) to reconstructed CMR images and the performance of either imaging by two separate operators, adding potential operator effects.

All together, some of these sources of disagreement between methods have a worse impact at end-systole than at end-diastole. Considering the naturally small values for ESV in normal rats, this explains the large relative difference in ESV and EF between methods (Tables 1, 2 and 4). As a result, the scatter of difference and the agreement interval for ESV and EF are wide in relative terms (Figure 3).

A third limitation appears to be the overestimation of volumes by HC-CMR compared to FV-CMR (Tables 1 and 2). Part of this overestimation may be related to the inclusion of portions of the LV outflow tract in a HC calculation that uses the length of the long-axis. A fourth limitation of our study is the lack of a “gold standard” among our reference measurements. Although CMR provides full-volume measures of LV by 3D imaging without geometric assumptions, the status of CMR as a gold standard measure of LV volumes in rodents is not as ascertained as it is in humans[1]. Prunier et al.[2] pointed to variations in CMR measurements between studies, in which the sham rat groups had different values, indicating additional sources of technical variation in rodent cardiac CMR. Our values on infarcted rats depart from the ones obtained in a recent study[16]. However, in the absence of a “gold standard”, our study, along with a previous study on mice[11], reports concordant values from two independent and well-accepted imaging modalities. This concordance, in our view, favors the accuracy of our measurements from both modalities. Accurate measurement of absolute LV volumes is gaining importance in rodent experiments, since the stroke volume is often used as a calibrator for LV volume measurement by conductance catheters[28], and validation studies like ours are best suited to generate reference values and ranges.

Acknowledgments

Grant and other support:

This work was supported by Leducq Foundation through the Caerus Network, by Centro Nacional de Investigaciones Cardiovasculares (CNIC) through the Cardio-Image program (TA) and by NIH R01 HL093183, HL088434, HL071763, HL080498, HL083156, and P20HL100396 (RJH) and NIH-T32-HL007824 (ERC).

References

[1]. Greupner J, Zimmermann E, Grohmann A, Dubel HP, Althoff T, Borges AC, et al. Head-to-Head Comparison of Left Ventricular Function Assessment with 64-Row Computed Tomography, Biplane Left Cineventriculography, and Both 2- and 3-Dimensional Transthoracic Echocardiography: Comparison With Magnetic Resonance Imaging as the Reference Standard. J Am Coll Cardiol. 2012; 59:1897–907. [PubMed: 22595410]

[2]. Prunier F, Marescaux L, Franconi F, Thia A, Legras P, Lejeune JJ, et al. Serial magnetic resonance imaging based assessment of the early effects of an ACE inhibitor on postinfarction left ventricular remodeling in rats. Can J Physiol Pharmacol. 2005; 83:1109–15. [PubMed: 16462910]

[3]. Pai RG, Varadarajan P. Echocardiography and cardiovascular magnetic resonance: evolution as complementary imaging tools. Curr Cardiol Rep. 2006; 8:155–7. [PubMed: 17543241]

[4]. Reffelmann T, Kloner RA. Transthoracic echocardiography in rats. Evalution of commonly used indices of left ventricular dimensions, contractile performance, and hypertrophy in a genetic model of hypertrophic heart failure (SHHF-Mcc-facp-Rats) in comparison with Wistar rats during aging. Basic Res Cardiol. 2003; 98:275–84. [PubMed: 12955400]

[5]. Prunier F, Pfister O, Hadri L, Liang L, Del Monte F, Liao R, et al. Delayed erythropoietin therapy reduces post-MI cardiac remodeling only at a dose that mobilizes endothelial progenitor cells. Am J Physiol Heart Circ Physiol. 2007; 292:H522–9. [PubMed: 16997893]

[6]. Chen J, Chemaly E, Liang L, Kho C, Lee A, Park J, et al. Effects of CXCR4 gene transfer on cardiac function after ischemia-reperfusion injury. Am J Pathol. 2010; 176:1705–15. [PubMed: 20133817]

[7]. Tournoux F, Petersen B, Thibault H, Zou L, Raher MJ, Kurtz B, et al. Validation of noninvasive measurements of cardiac output in mice using echocardiography. J Am Soc Echocardiogr. 2011; 24:465–70. [PubMed: 21315557]

[8]. Bunck AC, Engelen MA, Schnackenburg B, Furkert J, Bremer C, Heindel W, et al. Feasibility of functional cardiac MR imaging in mice using a clinical 3 Tesla whole body scanner. Invest Radiol. 2009; 44:749–56. [PubMed: 19838122]

[9]. Burri MV, Gupta D, Kerber RE, Weiss RM. Review of novel clinical applications of advanced, real-time, 3-dimensional echocardiography. Transl Res. 2012; 159:149–64. [PubMed: 22340764]

[10]. Scherrer-Crosbie M, Steudel W, Hunziker PR, Liel-Cohen N, Ullrich R, Zapol WM, et al. Three-dimensional echocardiographic assessment of left ventricular wall motion abnormalities in mouse myocardial infarction. J Am Soc Echocardiogr. 1999; 12:834–40. [PubMed: 10511652]

[11]. Dawson D, Lygate CA, Saunders J, Schneider JE, Ye X, Hulbert K, et al. Quantitative 3-dimensional echocardiography for accurate and rapid cardiac phenotype characterization in mice. Circulation. 2004; 110:1632–7. [PubMed: 15364813]

[12]. Ram R, Mickelsen DM, Theodoropoulos C, Blaxall BC. New approaches in small animal echocardiography: imaging the sounds of silence. Am J Physiol Heart Circ Physiol. 2011; 301:H1765–80. [PubMed: 21873501]

[13]. Picard MH, Popp RL, Weyman AE. Assessment of left ventricular function by echocardiography: a technique in evolution. J Am Soc Echocardiogr. 2008; 21:14–21. [PubMed: 18165124]

[14]. Isgaard J, Kujacic V, Jennische E, Holmang A, Sun XY, Hedner T, et al. Growth hormone improves cardiac function in rats with experimental myocardial infarction. Eur J Clin Invest. 1997; 27:517–25. [PubMed: 9229233]

[15]. Chemaly ER, Hadri L, Zhang S, Kim M, Kohlbrenner E, Sheng J, et al. Long-term in vivo resistin overexpression induces myocardial dysfunction and remodeling in rats. J Mol Cell Cardiol. 2011; 51:144–55. [PubMed: 21549710]

[16]. van de Weijer T, van Ewijk PA, Zandbergen HR Slenter JM, Kessels AG, Wildberger JE, et al. Geometrical models for cardiac MRI in rodents: comparison of quantification of left ventricular

volumes and function by various geometrical models with a full-volume MRI data set in rodents. Am J Physiol Heart Circ Physiol. 2012; 302:H709–15. [PubMed: 22101529]

[17]. Gueret P, Meerbaum S, Zwehl W, Wyatt HL, Davidson RM, Uchiyama T, et al. Two-dimensional echocardiographic assessment of left ventricular stroke volume: experimental correlation with thermodilution and cineangiography in normal and ischemic states. Cathet Cardiovasc Diagn. 1981; 7:247–58. [PubMed: 7285103]

[18]. Lang RM, Bierig M, Devereux RB, Flachskampf FA, Foster E, Pellikka PA, et al. Recommendations for chamber quantification: a report from the American Society of Echocardiography's Guidelines and Standards Committee and the Chamber Quantification Writing Group, developed in conjunction with the European Association of Echocardiography, a branch of the European Society of Cardiology. J Am Soc Echocardiogr. 2005; 18:1440–63. [PubMed: 16376782]

[19]. Chen J, Chemaly ER, Liang LF, LaRocca TJ, Yaniz-Galende E, Hajjar RJ. A new model of congestive heart failure in rats. Am J Physiol Heart Circ Physiol. 2011; 301:H994–1003. [PubMed: 21685270]

[20]. Stein AB, Tiwari S, Thomas P, Hunt G, Levent C, Stoddard MF, et al. Effects of anesthesia on echocardiographic assessment of left ventricular structure and function in rats. Basic Res Cardiol. 2007; 102:28–41. [PubMed: 17006633]

[21]. Coolen BF, Geelen T, Paulis LE, Nauerth A, Nicolay K, Strijkers GJ. Three-dimensional T1 mapping of the mouse heart using variable flip angle steady-state MR imaging. NMR Biomed. 2011; 24:154–62. [PubMed: 20960583]

[22]. Bland JM, Altman DG. Statistical methods for assessing agreement between two methods of clinical measurement. Lancet. 1986; 1:307–10. [PubMed: 2868172]

[23]. Russel IK, Gotte MJ, Bronzwaer JG, Knaapen P, Paulus WJ, van Rossum AC. Left ventricular torsion: an expanding role in the analysis of myocardial dysfunction. JACC Cardiovasc Imaging. 2009; 2:648–55. [PubMed: 19442954]

[24]. Stuckey DJ, Carr CA, Tyler DJ, Clarke K. Cine-MRI versus two-dimensional echocardiography to measure in vivo left ventricular function in rat heart. NMR Biomed. 2008; 21:765–72. [PubMed: 18457349]

[25]. Watson LE, Sheth M, Denyer RF, Dostal DE. Baseline echocardiographic values for adult male rats. J Am Soc Echocardiogr. 2004; 17:161–7. [PubMed: 14752491]

[26]. Xu Q, Ming Z, Dart AM, Du XJ. Optimizing dosage of ketamine and xylazine in murine echocardiography. Clin Exp Pharmacol Physiol. 2007; 34:499–507. [PubMed: 17439422]

[27]. Chemaly ER, Chaanine AH, Sakata S, Hajjar RJ. Stroke volume-to-wall stress ratio as a load-adjusted and stiffness-adjusted indicator of ventricular systolic performance in chronic loading. J Appl Physiol. 2012; 113:1267–84. [PubMed: 22923502]

[28]. Pacher P, Nagayama T, Mukhopadhyay P, Batkai S, Kass DA. Measurement of cardiac function using pressure-volume conductance catheter technique in mice and rats. Nat Protoc. 2008; 3:1422–34. [PubMed: 18772869]

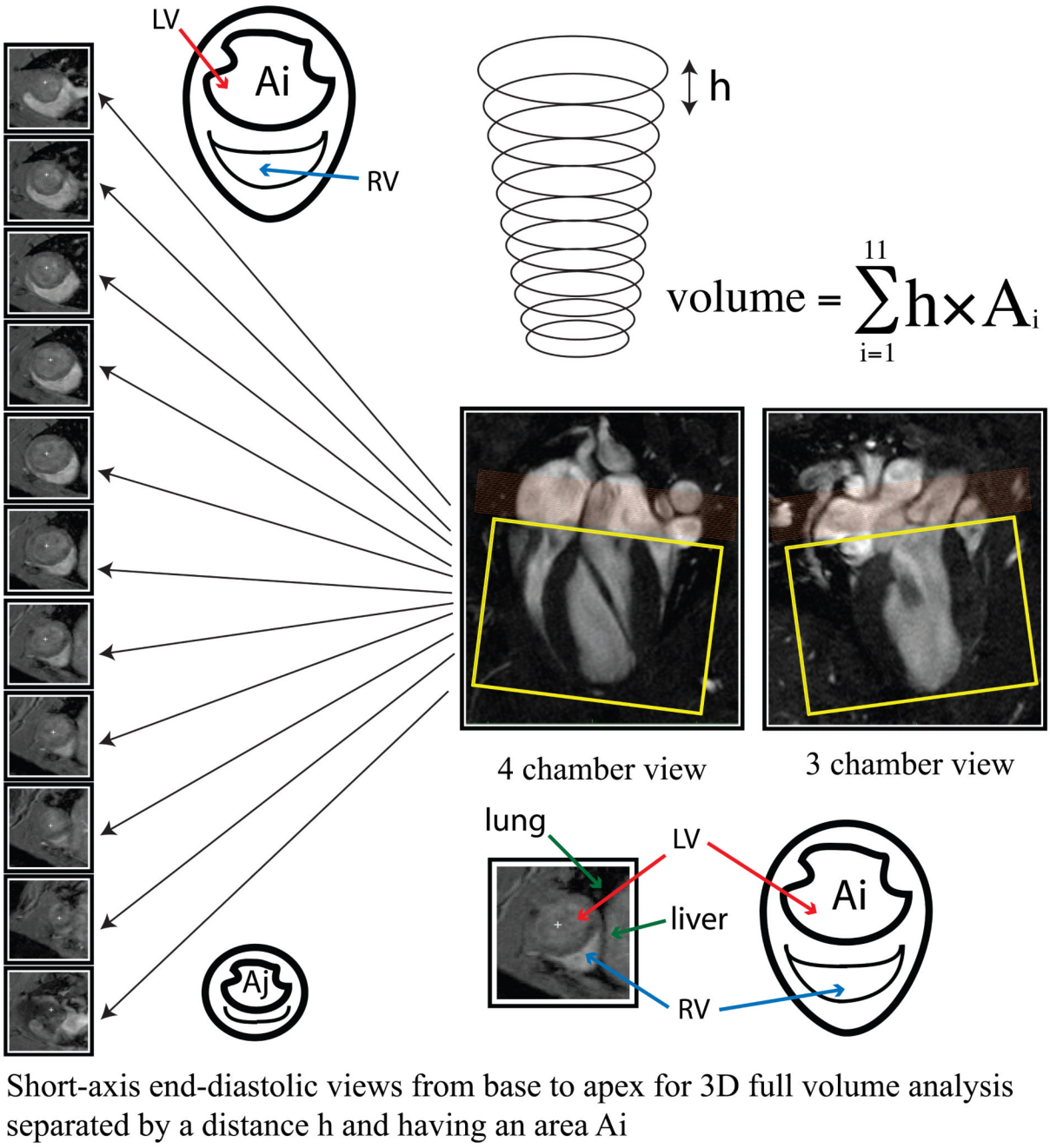

Figure 1.
Corresponding 4 chamber and 3 chamber views of the LV by CMR along with serial short-axis views used for full-volume analysis. Orange rectangle: navigator slice, yellow rectangle: 3D imaging package. Serial short-axis views with an area A_i and separated by a distance h are accounted for in the Simpson's full volume calculation.

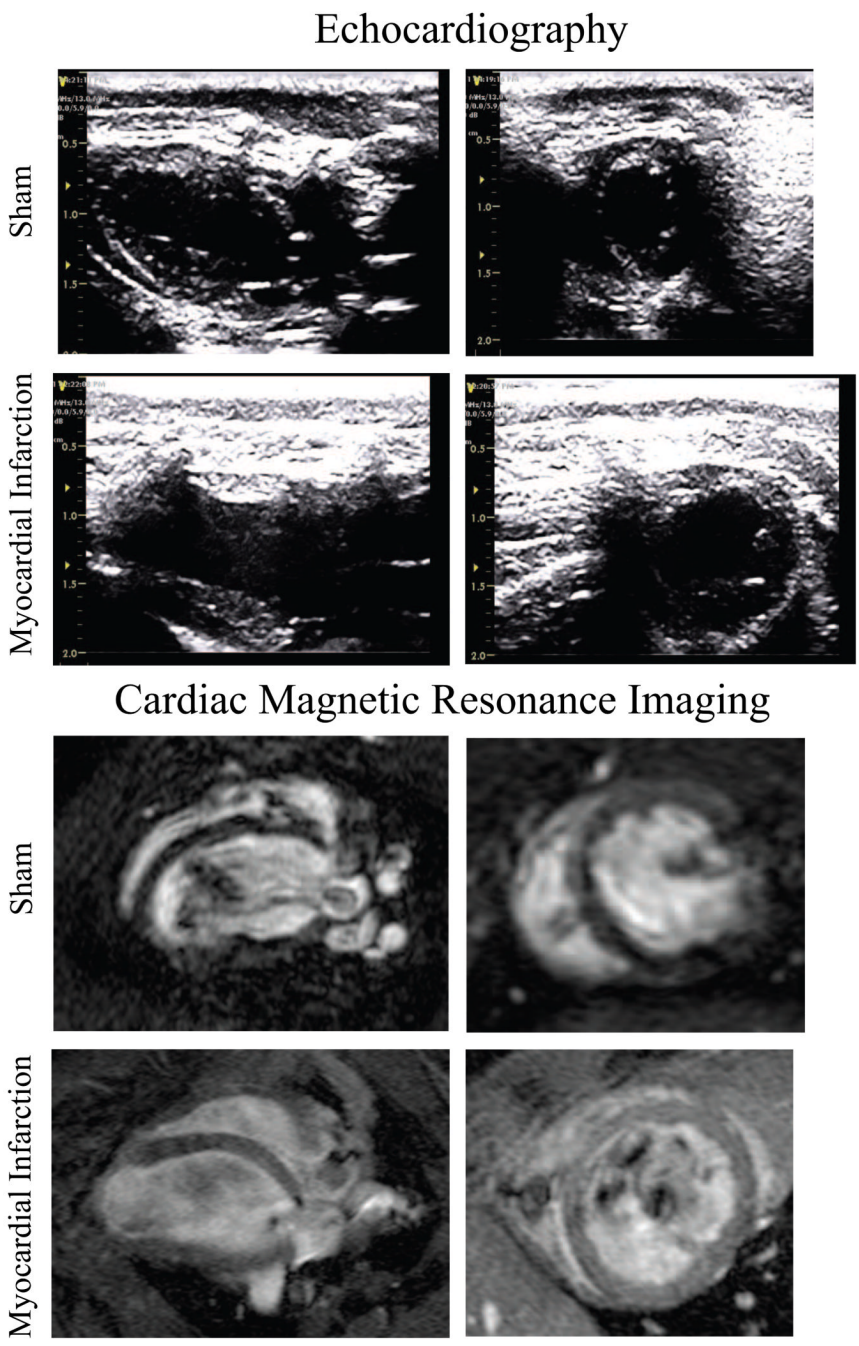

Figure 2.
Corresponding long-axis and short-axis views of the LV by echocardiography, with 4 chamber and short-axis CMR on representative sham and post-myocardial infarction rats.

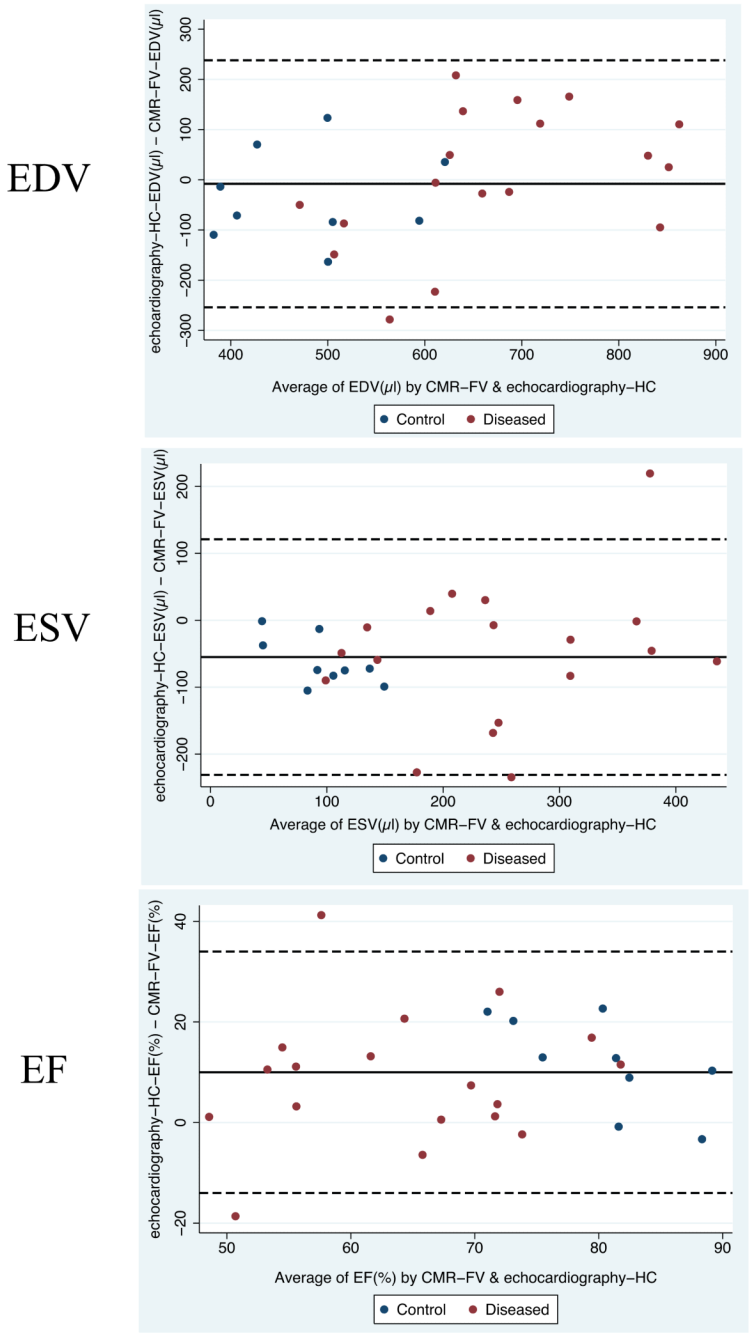

Figure 3.

Bland-Altman plots of LV end-diastolic volume (EDV), end-systolic volume (ESV) and ejection fraction (EF) by hemisphere-cylinder (HC) echocardiography vs. full-volume CMR (CMR-FV).

Blue dots represent control animals (normal and sham groups) and red dots represent diseased animals. Solid horizontal lines represent the mean difference between methods, and dashed lines are the 95% confidence limits of the difference (mean±2 standard deviations). Results of paired analysis (paired t-tests) are shown in Table 2.

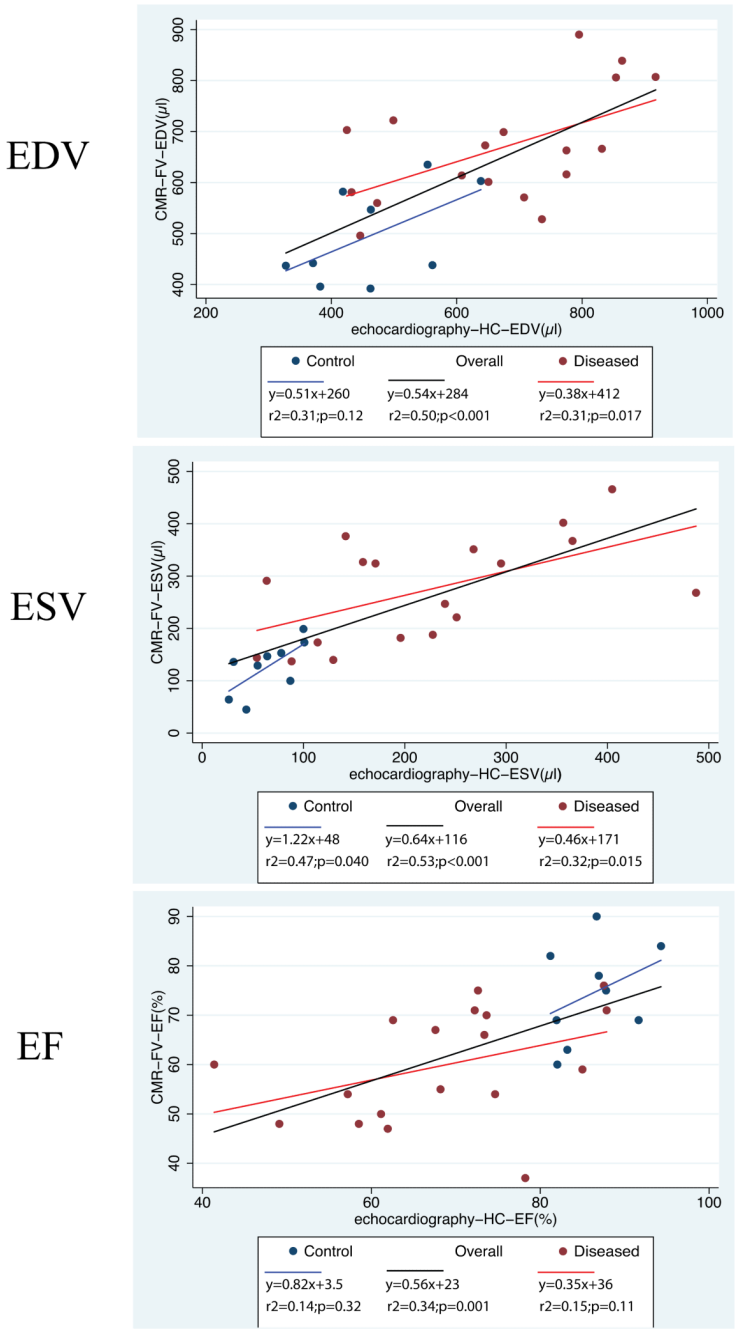

Figure 4.

Scatter-plots with linear regression fit of LV end-diastolic volume (EDV), end-systolic volume (ESV) and ejection fraction (EF) by full-volume CMR (CMR-FV) vs. hemisphere-cylinder (HC) echocardiography. Blue color is used for control animals (normal and sham groups) and red color for diseased animals, with the black linear regression line drawn for the overall (n=27) study sample.

Table 1

LV volumes and function by animal group measured by echocardiography (HC) and CMR (HC and FV)

	EDV (µl)			ESV (µl)			EF (%)			HR (bpm)	
Group	**Echo-HC**	**CMR-HC**	**CMR-FV**	**Echo-HC**	**CMR-HC**	**CMR-FV**	**Echo-HC**	**CMR-HC**	**CMR-FV**	**Echo**	**CMR**
Apical MI n=11	706±160*	1250±228	729±94 ***##§	262±129*#	491±80 ***###§§§ΨΨ	328±77***###§Ψ	64±13 **#	60±6 **###§§§	55±10 *#	403±53	284±53
POH n=4	666±149	1031±137 (n=3)	553±52	158±109	195±26 (n=3)	197±87	78±12	81±4 (n=3)	65±13	324±44	309±41
Small apical MI n=3	560±187	1022±108	601±54	165±75	318±17	178±41	71±3	69±3	71±4	404±38	298±78
Normal n=5	509±119	1045±179	532±92	82±23	244±60	134±62	84±3	77±3	75±12	404±50	271±59
Sham n=4	409±41	953±36 (n=3)	453±89	44±18	249±5 (n=3)	119±37	89±5	74±1 (n=3)	74±9	417±36	332±47
p for ANOVA	0.013	0.079	0.0001	0.005	<0.0001	<0.0001	0.002	<0.0001	0.006	0.069	0.50

CMR, cardiac magnetic resonance imaging; Echo, echocardiography; EDV, end-diastolic volume; EF, ejection fraction; ESV, end-systolic volume; FV, full volume CMR (see text); HC, hemisphere-cylinder formula (see text); HR, heart rate; MI, myocardial infarction; POH, pressure overload hypertrophy and SD, standard deviation. Values are expressed as mean ± SD. Statistical comparisons are made between groups, and not between imaging modalities.

p-values for Apical MI vs. Sham:

* p<0.05

** p<0.01

*** p<0.001

**** p<0.0001

p-values for Apical MI vs. Normal:

# p<0.05

p<0.01

p<0.001

p-values for Apical MI vs. POH:

§ p<0.05

§§§ p<0.001

p-values for Apical MI vs. Small apical MI:

Ψ p<0.05

Table 2

Paired comparison of echocardiography (HC) and CMR (HC and FV) for EDV, ESV and EF in diseased and non-diseased animals separately, and for the whole study sample

	EDV (μl)			ESV (μl)			EF (%)		
	Echo-HC	**CMR-HC**	**CMR-FV**	**Echo-HC**	**CMR-HC**	**CMR-FV**	**Echo-HC**	**CMR-HC**	**CMR-FV**
Diseased n=18	673±161 ****	1171±220 (n =17)§§§§	669±111	223±123 ****	408±137 (n =17) §§§§	274±100	68±13 #	65±9 (n =17) §	60±11
Normal and sham n=9	464±102 ****	1011±144 (n=8) §§§§	497±94	65±28 ###****	246±45 (n=8) §§§§	127±50	86±5 ##**	76±3 (n=8)	74±10
Overall n=27	603±174 ****	1120±210 (n=25) §§§§	611±133	170±126 ##****	356±138 (n=25) §§§§	225±111	74±14###**	69±9 (n=25) §	65±13

CMR, cardiac magnetic resonance imaging; Echo, echocardiography; EDV, end-diastolic volume; EF, ejection fraction; ESV, end-systolic volume; FV, full volume; HC, hemisphere-cylinder and SD, standard deviation.

Values are expressed as mean ± SD. Only significant p-values for paired t-tests are reported as follows:

p-values for Echo-HC vs. CMR-HC:

* p<0.05

** p<0.01

*** p<0.001

**** p<0.0001

p-values for Echo-HC vs. CMR-FV:

# p<0.05

p<0.01

p<0.001

p-values for CMR-HC vs. CMR-FV:

§ p<0.05

§§ p<0.01

§§§ p<0.001

§§§§ p<0.0001

Table 3

Comparison of LV mid-papillary short-axis area and LV long-axis length as measured by echocardiography and CMR

	Short-axis area (cm^2)				Long-axis length (cm)			
	End-diastole		End-systole		End-diastole		End-systole	
Imaging modality	**Echo**	**CMR**	**Echo**	**CMR**	**Echo**	**CMR**	**Echo**	**CMR**
Diseased n=18	0.46±0.10 ****	0.78±0.11	0.17±0.09 ****	0.31±0.09	1.77±0.11	1.80±0.13 (n=17)	1.57±0.17	1.59±0.19 (n=17)
Normal and sham n=9	0.35±0.06 ****	0.68±0.08	0.06±0.03 ****	0.23±0.05	1.56±0.13 ****	1.73±0.13 (n=8)	1.20±0.10	1.20±0.09 (n=8)
Overall n=27	0.42±0.10 ****	0.75±0.11	0.13±0.09 ****	0.28±0.09	1.70±0.15 **	1.77±0.13 (n=25)	1.45±0.23	1.46±0.25 (n=25)

CMR, cardiac magnetic resonance imaging; Echo, echocardiography and SD, standard deviation.

Values are expressed as mean ± SD. Only significant p-values for paired t-tests (Echo vs. CMR) are reported as follows:

* $p<0.05$

** $p<0.01$

*** $p<0.001$

**** $p\leq0.0001$

Table 4

Echocardiographic EDV and ESV using a modified Simpson rule and a single-plane ellipsoid area-length formula applied to the parasternal long-axis view (see text for details). In contrast with the hemisphere-cylinder (HC) model (Tables 1 and 2), significant and marked underestimation of EDV is observed versus full-volume (FV) CMR.

	EDV (μl)			ESV (μl)		
	Echo-Simpson	**Echo-Area-Length**	**CMR-FV**	**Echo-Simpson**	**Echo-Area-Length**	**CMR-FV**
Diseased n=18	511±130 ***	538±140 **	669±111	199±104 **	217±118 *	274±100
Normal and sham n=9	397±71 **	418±75 *	497±94	60±16 **	68±15 **	127±50
Overall n=27	473±125 ****	498±133 ***	611±133	153±108 ***	167±120 **	225±111

CMR, cardiac magnetic resonance imaging; Echo, echocardiography; EDV, end-diastolic volume; ESV, end-systolic volume; FV, full-volume and SD, standard deviation.

Values are expressed as mean ± SD. Only significant p-values for paired t-tests (vs. CMR-FV) are reported as follows:

* p<0.05

** p<0.01

*** p<0.001

**** p<0.0001

Table 5

Echocardiography using the hemisphere-cylinder (HC) formula and full-volume (FV) CMR are compared in their ability to detect changes (Δ) in EDV, ESV and EF from a reference value, which is the average value of the control group in Table 2.

	ΔEDV(μl)		ΔESV(μl)		ΔEF(%)	
	Echo-HC	**CMR-FV**	**Echo-HC**	**CMR-FV**	**Echo-HC**	**CMR-FV**
Reference value	464	497	65	127	86	74
Apical MI n=11	242±160	232±94	197±129	201±77	−22±13	−19±10
POH n=4	202±149	56±52	93±109	70±87	−8±12	−9±13
Small apical MI n=3	96±187	104±54	100±75	51±41	−15±3 *	−3±4
All diseased rats n=18	209±161	172±111	158±123	147±100	−18±13	−14±11

CMR, cardiac magnetic resonance imaging; Echo, echocardiography; EDV, end-diastolic volume; ESV, end-systolic volume; FV, full-volume and SD, standard deviation.

Values are expressed as mean ± SD.

* $p<0.05$ by paired t-test vs. CMR-FV